Ku- and C-Band SAR for Discriminating Agricultural Crop and Soil Conditions

M. Susan Moran, Alain Vidal, Denis Troufleau, Yoshio Inoue, and Thomas A. Mitchell

Abstract— **A method is proposed to estimate both green leaf area index (GLAI) and soil moisture (h_v), based on radar measurements at the Ku-band (14.85 GHz) and C-band (5.35 GHz) frequencies. The Ku-band backscatter at large incidence angles was found to be independent of soil moisture conditions and could be used alone to estimate GLAI. Then, the Ku-band estimate of GLAI could be used with a measurement of C-band backscatter in a canopy radiative transfer model to isolate the value of h_v. This concept was demonstrated with a set of Ku- and C-band synthetic aperture radar (SAR) backscatter data acquired over agricultural fields in Arizona. The demonstration showed promise for operational application of the method, though several limitations were identified. Since both Ku- and C-band σ^o are sensitive to soil roughness, this approach must be applied only to fields of similar soil roughness or row direction. This limitation may be less serious for farm management applications since crop type and cultivation practices are generally well known and can be taken into consideration. Another limitation of the use of Ku- and C-band σ^o is the apparent saturation of the Ku-band signal with increasing GLAI. Operational implementation of this approach will require dual-frequency sensors aboard an aircraft or orbiting satellite.**

Index Terms—**Agriculture, airborne radar, radar applications, radar imaging/mapping, remote sensing, satellite applications, soil measurements, synthetic aperture radar, vegetation.**

I. Introduction

SEVERAL recent studies in mapping soil moisture conditions of agricultural fields have suggested that a combination of high- and low-frequency synthetic aperture radar (SAR) could be used to determine the vegetation-induced attenuation of the low-frequency signal and improve estimates of soil moisture [1]–[3]. There is some evidence that the microwave signal at high frequencies (e.g., 10 GHz) is primarily sensitive to such plant parameters as green leaf area index (GLAI), plant biomass, and percent vegetation cover [4]. At lower frequencies (e.g., 5.3 GHz), there is evidence that the backscatter signal is very sensitive to soil moisture [5]–[9]. However, both low- and high-frequency data can also be very sensitive to soil roughness [10]–[12] and the low-frequency signal can be attenuated by increasing vegetation cover, thus, decreasing its sensitivity to soil moisture conditions [13]. These complications have restricted the use of microwave data for mapping soil moisture conditions of heterogeneous, natural landscapes. Fortunately, these complications are less restrictive for farm management applications where field conditions are generally well known (e.g., planting date, crop type, soil cultivation practices, etc.).

In this work, we propose that an algorithm could be developed for farm-scale agricultural applications to estimate GLAI and soil moisture (h_v), based on radar measurements at the Ku-band (14.85 GHz) and C-band (5.35 GHz) frequencies. This is based on evidence that the Ku-band at large incidence angles is independent of soil moisture conditions and sensitive to GLAI [14] and thus, could be used alone to estimate GLAI. The C-band backscatter at small incidence angles is very sensitive to soil moisture conditions, but is also attenuated by increasing GLAI [10]. Thus, the Ku-band estimate of GLAI could be used with a measurement of C-band backscatter in a canopy model to isolate the value of h_v. The modeled results could be used to construct a mesh graph, whose Cartesian coordinates would be related to crop growth and soil water conditions. Then, the location of field measurements of SAR backscatter could be plotted within the mesh graph and used to estimate the soil moisture and GLAI of each field. This approach was applied with some success with active and passive microwave data to determine soil wetness and surface roughness [15].

The objective of this study was to demonstrate this approach by using a data set of Ku- and C-band SAR backscatter acquired over cotton and alfalfa fields in Arizona. We used the parametric water cloud model [16] with revisions made by Prevot *et al.* [2] to construct the mesh graph. The final results were a comparison of the modeled soil moisture estimates with actual field measurements and the production of maps of soil moisture and GLAI for an agricultural center.

II. Water Cloud Model

The general water-cloud model represents the power backscattered by the whole canopy σ^o as the sum of the contribution of the vegetation σ_v^o and that of the underlying soil σ_s^o. The latter is attenuated by the vegetation layer. Thus, for a given incidence angle (θ)

$$\sigma^o = \sigma_v^o + \tau^2 \sigma_s^o \text{ (units: } \mathrm{m^2/m^2}) \tag{1}$$

where

$$\sigma_v^o = A V_1^E \cos\theta (1 - \tau^2) \text{ (units: } \mathrm{m^2/m^2}) \tag{2}$$

$$\sigma_s^o = C + D h_v \text{ (units: dB)} \tag{3}$$

Manuscript received May 31, 1996; revised February 21, 1997. This work was supported by the National Science Foundation (INT-9314872) and a cooperative grant from the Japanese government.

M. S. Moran and T. A. Mitchell are with the USDA-ARS U.S. Water Conservation Laboratory, Phoenix, AZ 85040 USA (e-mail: moran@tucson.ars.ag.gov).

A. Vidal and D. Troufleau are with the Cemagref-ENGREF Remote Sensing Research Laboratory, Montpellier, France.

Y. Inoue is with the NIAES Laboratory of Agro-Biological Measurements, Tsukuba, Japan.

Publisher Item Identifier S 0196-2892(98)00144-2.

0196–2892/98$10.00 © 1998 IEEE

h_v is volumetric soil moisture content (cm^3/cm^3), and V_1 is a descriptor of the canopy. τ^2 is the two-way attenuation through the canopy, expressed as

$$\tau^2 = \exp(-2BV_2/\cos\theta) \text{ (unitless)} \quad (4)$$

where V_2 is a second canopy descriptor. The canopy descriptors (V_1 and V_2) in (2) and (4) have been associated with GLAI [2], [10], so for this application we assumed $V_1 = V_2 = \text{GLAI}$.

The coefficients D and C can be determined based on a linear regression of σ^o with h_v measured for a bare soil field over a drying period. Values for A, B, and E (and C, if necessary) can be determined by fixing D and minimizing the sum of squares of the differences between modeled and measured σ^o based on (1)–(4), where

$$\sigma^o = (AV_1^E \cos\theta\{1 - [\exp(-2BV_2/\cos\theta)]\}) + \{\exp(-2BV_2/\cos\theta)\sigma_s^o\} \text{ (units: } m^2/m^2) \quad (5)$$

and σ_s^o is evaluated with (3) and converted from units of decibels to m^2/m^2.

TABLE I
MODEL PARAMETER ESTIMATIONS FOR (1)–(5) BASED ON RESULTS FOR WHEAT GIVEN BY PREVOT *et al.* [2] AND THOSE USED FOR THIS CONCEPT DEMONSTRATION AT MAC

Radar configuration			Vegetation Parameters			Soil Parameters	
			A	B	E	C	D
Prevot et al. (1993)							
C-band	Mean	Wht	0.000	0.089	0.00	-4.50	19.20
20°,HH	SD		-	0.013	-	0.78	-
X-band	Mean		0.021	0.417	0.99	-14.00	19.20
40°,VV	SD		0.044	0.114	0.11	0.92	-
MAC Results 1994/95			A	B	E	C	D
C-band	Mean	CE:	0.000	0.09	0.00	-11	27.8
23°,VV		CN:	0.000	0.09	0.00	-8.5	27.8
		Alf:	0.000	0.09	0.00	-13	27.8
Ku-band	Mean	CE:	0.048	0.8	1.0	-12	0.0
55°,VV		CN:	0.125	0.8	1.0	-10.7	0.0
		Alf:	0.030	0.8	1.0	-14	0.0

III. SPECTRAL AND FIELD DATA

Results from two measurement campaigns were used to demonstrate the integration of dual-frequency microwave data and the water cloud model. During both campaigns (June 1994 and April 1995), near-simultaneous images in the Ku- and C-band SAR frequencies were acquired over the Maricopa Agricultural Center (MAC) near Phoenix, AZ. During the June campaign, the predominant crops were alfalfa (near full cover) and cotton (near 40% cover). During April, the cotton had been planted but the first leaves had only just emerged; the alfalfa was near the same stage of growth as alfalfa in June 1994. Since the predominant irrigation method for MAC is flooding, each field is dissected into a number of level basins. These within-field basins are generally termed "borders" and that terminology will be used hereon. During a single irrigation, the borders are sequentially flooded with a three-to-four day progression from one end of a 1.6-km field to the other.

European Remote Sensing (ERS-1) satellite SAR images [C-band (5.35 GHz), VV polarization, and 23° incidence angle] covering most of MAC were obtained on June 15, 1994 and April 25, 1995. The digital numbers (dn) were converted to a backscattering coefficient expressed in decibels by using the SAR calibration coefficient (T. Lukowski, Canadian Centre for Remote Sensing, personal communication). Images of MAC from an airborne SAR sensor [Ku-band (14.85 GHz), VV polarization, and 55° incidence angle] were provided on June 24, 1994 and April 27, 1995 (12 pm MST) by Sandia National Laboratories (SNL), Albuquerque, NM. The aircraft-based SAR dn was expressed in decibels, based on the calibration coefficient (J. Bradley, SNL, personal communication), with an estimated calibration error of 1.2 dB.

Values of C-band and Ku-band σ^o from the ERS-1 and SNL sensors were averaged to one value for each irrigation border. The number of pixels averaged varied with the size of the border. For the coarsest-resolution data, ERS-1 SAR, the number of pixels averaged ranged from 14 pixels for the smallest border to 100 pixels for the largest. For the finest resolution data SNL SAR, the number of pixels averaged for each border was well over 1000.

During each overpass, a survey of the farm was conducted to record border-by-border visual estimates of crop height, vegetation cover (V_c), soil roughness, and soil moisture (Table II). In addition to the visual surveys, detailed vegetation measurements were made in selected cotton and alfalfa fields on a weekly basis during the cotton growing season in 1994 and on April 24, 1995. In five 2-m^2 sample sites within selected cotton field borders, measurements were made of plant density, height, V_c, and number of squares/bolls/flowers. In five 0.5-m^2 sample sites within selected alfalfa field borders, plant density, height and percent cover were measured.

During the June overpasses, the cotton and alfalfa fields were at varying stages of irrigation with borders ranging from very dry to near-field capacity. Gravimetric soil moisture samples to 5-cm depth were made in selected fields. Several values were averaged to produce one estimate of soil moisture content for each of the selected borders. During the April overpass, all the cotton fields were dry (no irrigation or precipitation for four weeks prior). In two cotton fields with north–south (NS) and east–west (EW) row orientations, we flooded areas the size of several borders (~0.2 × 0.2 km). Measurements of soil moistures were made in the dry and saturated parts of these fields during the SAR overpasses. Since the fields were virtually bare, these areas could be used to evaluate the sensitivities of Ku- and C-band σ^o to soil moisture (3) in fields with NS and EW row orientations.

IV. RESULTS AND DISCUSSION

The following sections present results of the calibration of the water cloud model based on field measurements at MAC and construction of the Ku- and C-band mesh graph. Field measurements from the April experiment (when cotton fields were furrowed but only the plant cotyledons were exposed) were used to compute the model coefficients C and D,

TABLE II
MAC FIELD CONDITIONS ACCORDING TO THE VISUAL FIELD SURVEY CONDUCTED ON DOY 165. F# REFERS TO THE MAC FIELD NUMBER AND REFERENCES TO B# WITHIN THE TABLE REFERS TO THE BORDER (LEVEL IRRIGATION BASIN) NUMBER WITHIN THE FIELD

F#	Crop Type	Soil Roughness	Vegetation Height	Vegetation Cover (%)	Soil Moisture
11	Cotton	N/S rows, raked	B1-3: 8 mm	B1-3: 45	Moist
13	Cotton	N/S rows, raked	B1-6: 8 mm B7-8: 6 mm	B1-2: 60 B3-8: 50	B1: Moist B2-8: Wet
15	Alfalfa	Smooth	B1-16: 5 mm	B1-16: 80	B1: Wet B2-16: Water
17	Alfalfa	Smooth	B1-16: 5 mm	Ranging from 80% in B16 to 30% in B2	B1-6: Wet B7-10: Moist B11-16: Damp
19	Cotton	N/S rows, raked	B1: 7 mm B2-4: 6 mm	B1: 40 B2-4: 35	Dry
20	Cotton	N/S rows, raked	B1-3: 5 mm B4: 6mm	B1-3: 25 B4: 35	Dry

(a)

23	Cotton	N/S rows, not raked	B1-4: 8 mm	B1: 40 B2: 20 B3: 30 B4: 50	Dry
25	Alfalfa	Smooth	B1-16: 5 mm	50% in B2; 70-80% in all other borders	B1-5: Moist B6-9: Wet B10-16: Moist
31	Cotton	E/W rows, raked	B1-8: 7 mm	B1-8: 40	Dry
33	Cotton	E/W rows, raked	B1-4: 5 mm	B1-4: 35	Dry
34	Cotton	E/W rows, raked	B1: 6 mm B2-4: 7 mm	B1: 25 B2-4: 35	Dry
35	Cotton	E/W rows, raked	B1, B3, B5, B7: 6 mm All other: 3 mm	B1, B3, B5, B7: 30 All other: 10	B1: Water B2-B7: Moist
36	Cotton	E/W rows, raked	B3: 4mm All other: 6 mm	B3: 15 All other: 30	B1-3: Dry B4-7: Moist
37	Cotton	E/W rows, raked	B1-3: 6 mm B4: Mix	B1-3: 30 B4: Mix	Moist
38	Cotton	E/W rows, raked	B1, B4: 7 mm B2, B3: 6 mm	B1, B4: 35 B2,B3: 25	Dry

(b)

related to SAR signal sensitivity to soil moisture. The model coefficient E was set to 0.0 for the C-band and to 1.0 for the Ku-band, based on results published by Prevot *et al.* [2] for similar frequencies for wheat. This left only two model coefficients A and B, related to SAR signal sensitivity to vegetation. Field measurements from the June experiments (when soil and plant conditions varied) were used to estimate the model coefficients A and B.

We acknowledge several weaknesses in this calibration of the water cloud model: 1) the previously-published results for wheat were not necessarily applicable to cotton and alfalfa and 2) the estimation of A and B coefficients were based on a limited data set. Furthermore, in construction of the mesh graph, we combined Ku- and C-band data from acquisitions at different times of day and separated by ten days. Even though crop conditions were relatively unchanged in the fields over this ten-day period, there could certainly have been variations in physical or dielectric canopy conditions that affected the SAR signal. However, we feel these weaknesses will not necessarily defeat our objective, which was simply to demonstrate a concept. In fact, in application it would be preferable to use a physically based model (e.g., the integral equation model (IEM); [17]) rather than a parametric representation, such as the water cloud model. Since no physical information is used in defining the water cloud parameters, the model results can only be applied to a set of plant and soil characteristics identical to those used in calibration.

A. Sensitivity of Ku- and C-Band σ^o to Soil Moisture

The SAR measurements made in April 1995 for near-bare field conditions with dry and saturated soils were used to evaluate the C and D coefficients in (3). The slopes of C-band σ^o with h_v were 30.4 and 25.1 for Field 30 with NS rows and Field 26 with EW rows [Fig. 1(b)]. Based on these measurements, we assumed that the slope was a constant value equal to the average of these two measurements ($D = 27.8$) for all fields. For the cotton fields, we set the model coefficient C to an average of the C-band σ^o for all the furrowed fields in the NS and EW direction, respectively. This resulted in $C = -11$ for cotton with EW row orientation and $C = -8.5$ for cotton with NS rows. Since there was no information for the alfalfa fields because no bare soil conditions existed, the value of D was assumed constant ($D = 27.8$) and the value of C was assumed to be similar to other relatively smooth fallow fields in the image ($C = -13$).

From the measurements of Ku-band σ^o and h_v, it appeared that Ku-band σ^o had little to no sensitivity to soil moisture [Fig. 1(a)]. In fact, the signal decreased slightly with irrigation, possibly due to a decrease in the roughness of the soil associated with the irrigation. Based on this analysis, we assumed that the slope was zero ($D = 0$) and the intercept for the NS cotton, EW cotton, and alfalfa were equal to the values for dry, bare soil: -12, -10.7, and -14.0, respectively. The computation $D = 0$ was supported by analysis of the SAR Ku-band measurements during the June field campaigns (see [14, Fig. 7]).

B. Empirical Evaluation of Coefficients A and B

Since there were so few measurements of soil moisture and GLAI for the June and April experiments, it wasn't possible

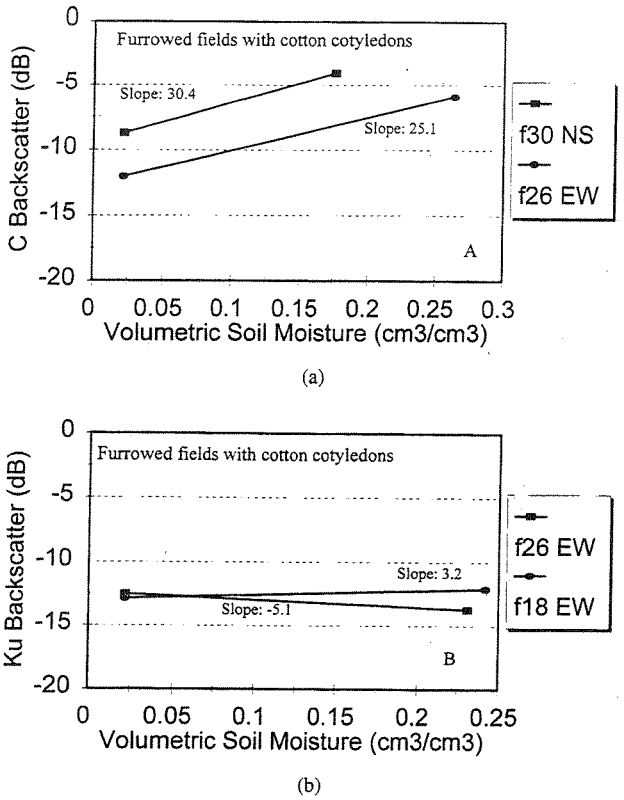

Fig. 1. Relation between volumetric soil moisture (@ 5 cm) and (a) C-band σ^o and (b) Ku-band σ^o based on measurements made during the April overpasses in cotton fields with EW and NS row orientations.

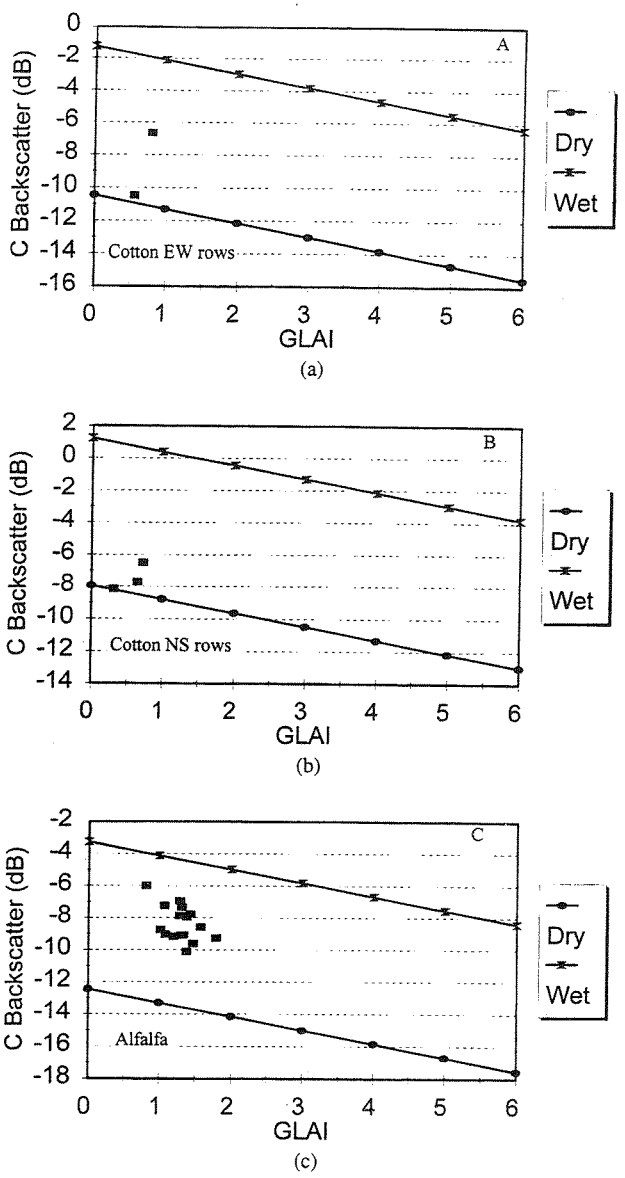

Fig. 2. Relation between GLAI and C-band SAR backscatter (σ^o) for (a) cotton with EW row orientation, (b) cotton NS row, and (c) alfalfa for dry (0.02) and wet (0.35) soil moisture conditions. The solid squares are measurements and the solid lines are the output from the water cloud model calibrated for C-band data by Prevot *et al.* [2].

to use the conventional, iterative approach for evaluating the coefficients A and B in (5). Instead, we set C and D equal to the values derived in the previous section (Table I) and used simplified methods to determine A and B. For the ERS-1 SAR C-band data, we used the evaluations of A and B for ERS-1 SAR data by Prevot *et al.* [2] for wheat. They found that A was 0.000 (implying that C-band σ_v was zero for all GLAI values) and the B value was set to 0.09, giving a value of transmittance of 0.88 at GLAI = 1.0. These values corresponded well with the behavior of the C-band data reported by Moran *et al.* [14] for cotton and alfalfa.

The modeled results for h_v values of 0.02 (labeled DRY in Fig. 2) and 0.35 (labeled WET) look reasonable, relative to C-band σ^o and GLAI values measured at MAC in June. That is, the measurements were encompassed between the modeled WET and DRY extremes with anticipated behavior. For example, the GLAI measurements in the cotton fields (NS rows) were classified as "dry" soils in the visual survey, and all three points are close the modeled DRY line. The GLAI measurements in the alfalfa fields were classified as "moist" to "wet" and they were located closer to the modeled WET line in Fig. 2.

For the Ku-band, we evaluated A and B by using the measurements of GLAI from fields of cotton and alfalfa at MAC. As reported in the previous section, the Ku-band was insensitive to soil moisture ($D = 0$), resulting in no difference between the modeled values for the DRY ($h_v = 0.02$) and WET ($h_v = 0.35$) soil conditions in Fig. 3. The best fit line between modeled and measured values was achieved with values of $B = 0.80$ and values of $A = 0.048$, 0.125, and 0.030 for EW cotton, NS cotton, and alfalfa, respectively (Table I).

In a similar study of dual-frequency microwave data, Prevot *et al.* [2] evaluated the water cloud model for C-band data (20°, HH) and X-band data (9.65 GHz, 40°, VV) acquired over a wheat canopy. Based on an iterative derivation of values A–E, they concluded the following.

1) Backscattering in C-band was represented as attenuation of the soil component by the canopy, as the vegetation contribution was negligible ($A = 0$).
2) The attenuation (B) and vegetation contribution itself (represented by A, B, and E) were larger in X-band than in C-band.
3) For the X band, when GLAI was high (GLAI > 4), the soil contribution was negligible and the backscattering was dominated by the vegetation contribution.

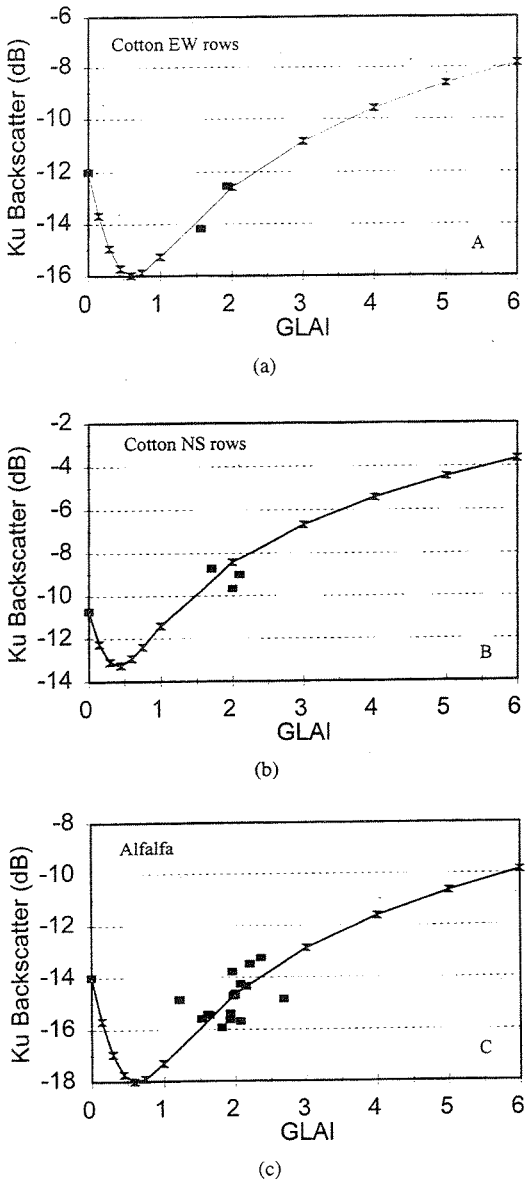

Fig. 3. Relation between GLAI and Ku-band SAR backscatter (σ^o) for (a) cotton with EW row orientation, (b) cotton NS row, and (c) alfalfa, independent of soil moisture conditions. The solid squares are measurements and the solid line is the output from the water cloud model calibrated to these data measurements.

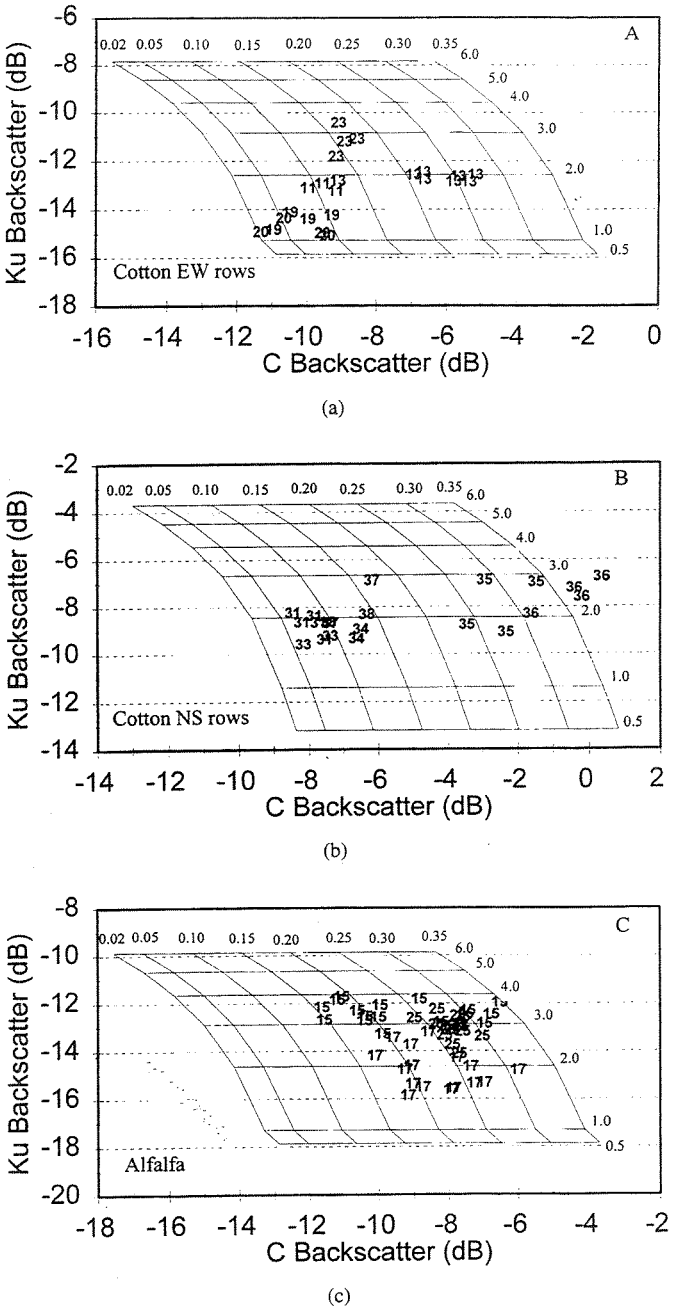

Fig. 4. Mesh graph of Ku- and C-band σ^o for (a) cotton with EW row orientation, (b) cotton NS row, and (c) alfalfa fields at MAC during the June overflights. The numbers represent field identifications and are used in lieu of solid markers for the locations of the Ku- and C-band σ^o measurements for border within each numbered field (Table II). The solid lines define modeled backscatter for values of GLAI (listed on the right) and soil moisture (listed on top), derived from the calibrated water cloud model.

Though we used the Ku-band frequency rather than the X-band frequency, our modeled and measured results for cotton and alfalfa support their findings for low- and high-frequency microwave backscatter from wheat. Additionally, we found the Ku-band SAR backscatter to be insensitive to variations in soil moisture ($D = 0$). This independence of the Ku- and C-band sensitivities lead to the hypothesis that a mesh graph of Ku- and C-band σ^o could allow discrimination of vegetation growth and soil moisture characteristics for farm management.

C. Computation and Validation of Mesh Graph Results

With the model coefficients listed in Table I, it was possible to compute Ku- and C-band σ^o values for varying combinations of GLAI and h_v. It is apparent from the trend in Fig. 3 that the relation between Ku-band σ^o and GLAI is only near-linear for values GLAI > 0.5. Thus, a simulated mesh graph was constructed for cotton and alfalfa over the range of $0.5 <$ GLAI < 6.0 and $0.02 < h_v < 0.35$ (the range of h_v values encountered during this experiment). The simulated mesh graph was superimposed over the scattergram of measured values of Ku- and C-band σ^o for all field borders during the June campaign (Fig. 4). The location of the measurements within the mesh graph were reasonable; that is, according to the visual surveys (Table II):

1) the wet fields were generally to right and dry fields to the left;

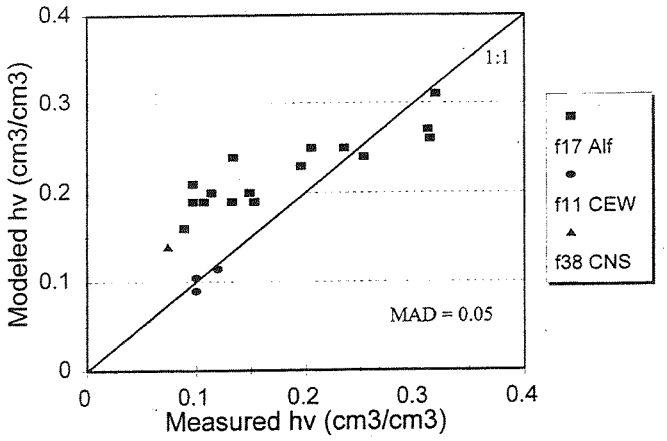

Fig. 5. Comparison of modeled and measured soil moisture (h_v) values within selected borders of three fields: Field 17 (alfalfa), Field 11 (cotton with EW rows), and Field 38 (cotton with NS rows).

2) fields with greater vegetation cover were located toward the top of the graph;
3) the GLAI and h_v values associated with Ku- and C-band σ^o were generally within the range of values measured on-site.

There is one exception that is a good illustration of the weakness of Ku-band SAR data for monitoring crop growth and vigor. In the visual survey (Table II), the soil moisture of Field 23 was classified as dry and vegetation cover was varied from 20 to 50%, similar to Fields 19 and 20. However, in the mesh graph, it is further right (indicating a moist soil, $h_v = 0.15$) and closer to the top (indicating an unreasonable GLAI = 3.0) than the measurements in Fields 19 and 20. Field 23 differed from the other cotton fields with EW rows in that the furrows were "not raked" and all others were "raked." This may have resulted in greater SAR backscatter in both the Ku and C bands (unrelated to increases in h_v and GLAI), thus distinguishing the results in Field 23 from other cotton fields in Fig. 4(a).

Another trend is the tendency of the measurements made in cotton with NS rows to indicate higher h_v values than expected [Fig. 4(b)]. Though the visual survey indicated that several fields were "dry," the lowest soil moisture were above 0.05 according to their location within the mesh. Also, the soil moisture values associated with Field 36 according to the mesh graph were greater than 0.35, which was the highest value we found in our measurements for all fields. This trend could indicate that the model coefficients we derived for cotton with NS rows (Table I) were not well suited.

A quantitative validation of the modeled results was conducted by using modeled and measured h_v values within selected border of three fields. Soil moisture measurements for borders within Fields 11, 17, and 38 were compared with modeled values derived from the mesh graph (Fig. 5). As expected, the one measurement made in the Field 38 (cotton with NS rows) was nearly half the modeled value (difference 0.07). For Field 11 (cotton with EW rows), the difference between modeled and measured values was within 0.01 cm^3/cm^3. For the alfalfa measurements which ranged from h_v = 0.1–0.32, the model tended to overestimate the lower values and underestimate the higher values, with differences varying from 0.11–0.01. Considering that the model calibration was accomplished with a very limited data set, these results are encouraging.

Images of GLAI and h_v were produced based on the mesh graph illustrated in Fig. 4, and the border-averaged values of Ku- and C-band σ^o derived from the ERS-1 and SNL images at MAC in June. These images illustrate the map products that could be produced from this simple, dual-frequency approach and could not be provided by either frequency alone.

V. Concluding Remarks

This approach is based on our findings that the Ku-band σ^o is sensitive to vegetation density and insensitive to soil moisture content, and the C-band σ^o is sensitive to soil moisture, though attenuated by increasing vegetation [14]. A mesh graph of Ku- and C-band σ^o showed some promise for estimation of both soil moisture and GLAI. This approach could be used operationally to produce maps of h_v and GLAI for agricultural areas and provide farm managers with information necessary to make decisions on water, fertilizer and insecticide applications.

There are limitations to this approach. Since both Ku- and C-band σ^o are sensitive to soil roughness [10], this approach must be applied only to fields of similar soil roughness or row direction. An example of the perils of combining different roughnesses is apparent in the 3–4 dB differences in Ku- and C-band σ^o for cotton fields of similar GLAI and h_v and different row directions [e.g., Fig. 1(b)]. This limitation may be less serious for farm management applications, since crop type and cultivation practices are generally well known and can be taken into consideration.

Another limitation of the use of Ku- and C-band σ^o is the apparent saturation of the Ku-band signal with increasing GLAI. Ulaby *et al.* [10] reported that, for GLAI > 2.0, σ^o_v at Ku-band frequency remained relatively constant though the GLAI increased to values as high as five and six for corn and sorghum. In our simulation of cotton and alfalfa backscatter, there was a noticeable decrease in the sensitivity of Ku-band σ^o to GLAI at GLAI > 4.0; the change in Ku-band σ^o associated with a change in GLAI from 5.0 to 6.0 was only 1 dB (Fig. 4). This is of the same magnitude as the error in instrument calibration and of smaller magnitude than the sensitivity to surface roughness, making the Ku signal appear saturated for general purposes. On the other hand, though the C-band signal decreased with increasing GLAI [13], the sensitivity to soil moisture condition ($\delta\sigma^o/\delta h_v$) remained relatively constant (Fig. 4).

There are two issues that should be considered in implementation of this concept. First, the results presented here were based on the use of Ku-band data obtained with a large incidence angle at midday, and C-band data obtained with a small incidence angle at night. Different results would be expected with different SAR configurations and overpass times. For example, though high-frequency Ku-band σ^o has been found to be sensitive to the soil moisture content of the top millimeter of soil [10], we found no sensitivity to soil

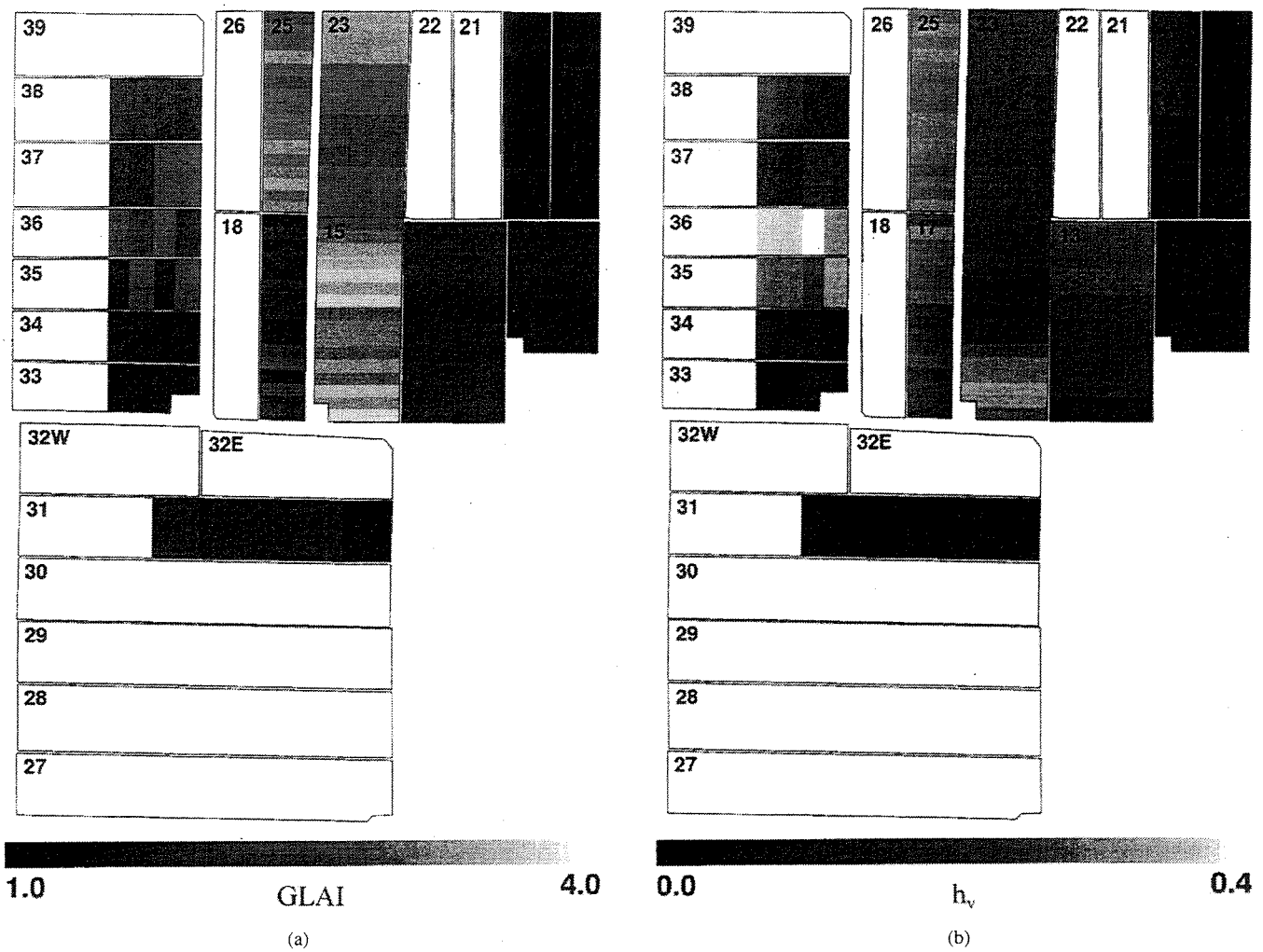

Fig. 6. Images of field GLAI and soil moisture (h_v) for Maricopa Agricultural Center (MAC), derived from Ku- and C-band backscatter measurements in relation to the mesh graph in Fig. 4.

moisture when the acquisition was made at large incidence angles at midday (when the top millimeter of even moist soils was dry). Furthermore, polarization can affect the sensitivity of the SAR signal to soil moisture conditions [13], and the size of the incidence angle has been correlated with sensitivity to surface roughness [18].

Second, from an operational point of view, at this time there are no Ku-band sensors nor any dual-frequency sensors aboard currently-orbiting satellites. Until such a sensor is available, an option that should be considered in implementation of this concept is the combination of ERS-1 C-band SAR data with visible and near-infrared (NIR) data acquired by SPOT or Landsat satellites as a substitute for the high-frequency Ku-band data. There is substantial evidence that vegetation indices based on the ratio of the red and NIR reflectance are very sensitive to GLAI [19] and could be used to determine the Y-axis in Fig. 4. Though this option is feasible, it circumvents the advantages of a SAR-only algorithm, such as acquisition of images during nighttime and cloudy conditions.

ACKNOWLEDGMENT

Images were provided by the European Space Agency, Sandia National Laboratories, and EG&G. The authors express particular appreciation to the Sandia AMPS team who worked with us to arrange the overflights and process the Ku-band SAR images. They also appreciate the cooperation and assistance of personnel at the Maricopa Agricultural Center (MAC) and USDA-ARS U.S. Water Conservation Laboratory.

REFERENCES

[1] O. Taconet, M. Benallegue, D. Vidal-Madjar, L. Prevot, M. Dechambre, and M. Normand, "Estimation of soil and crop parameters for wheat from airborne radar backscattering data in C and X bands," *Remote Sens. Environ.*, vol. 50, pp. 287–294, 1994.

[2] L. Prevot, I. Champion, and G. Guyot, "Estimating surface soil moisture and leaf area index of a wheat canopy using dual-frequency (C and X bands) scatterometer," *Remote Sens. Environ.*, vol. 46, pp. 331–339, 1993.

[3] S. Paloscia, P. Pampaloni, L. Chiarantini, P. Coppo, S. Gagliani, and G. Luzi, "Multifrequency passive microwave remote sensing of soil moisture and roughness," *Int. J. Remote Sens.*, vol. 14, pp. 467–483, 1993.

[4] B. A. M. Bouman, "Crop parameter estimation from ground-based X-band (3-cm wave) radar backscattering data," *Remote Sens. Environ.*, vol. 37, pp. 193–205, 1991.

[5] M. Benallegue, M. Normand, S. Galle, M. Dechambre, O. Taconet, D. Vidal-Madjar, and L. Prevot, "Soil moisture assessment at a basin scale using active microwave remote sensing: The Agriscatt'88 Airborne Campaign on the Orgeval Watershed," *Int. J. Remote Sensing*, vol. 15, pp. 645–656, 1994.

[6] P. Bertuzzi, A. Chanzy, D. Vidal-Madjar, and M. Autret, "The use of a microwave backscatter model for retrieving soil moisture over bare soil," *Int. J. Remote Sensing,* vol. 13, pp. 2653–2668, 1992.
[7] K. Dabrowska-Zielinska, Gruszcynska, M. Janowska, K. Stankiewicz, and Z. Bochenek, "Use of ERS-1 SAR data for soil moisture assessment," in *Proc. 2nd Euro-Latin Amer. Space Days,* Buenos Aires, Argentina, May 9–13, 1994, pp. 79–84.
[8] D. S. Lin, E. F. Wood, K. Beven, and S. Saatchi, "Soil moisture estimation over grass-covered areas using AIRSAR," *Int. J. Remote Sensing,* vol. 15, pp. 2323–2343, 1994.
[9] C. Schmullius and R. Furrer, "Frequency dependence of radar backscattering under different moisture conditions of vegetation-covered soil," *Int. J. Remote Sensing,* vol. 13, pp. 2233–2245, 1992.
[10] F. T. Ulaby, C. T. Allen, G. Eger, III, and E. Kanemasu, "Relating the microwave backscattering coefficient to leaf area index," *Remote Sens. Environ.,* vol. 14, pp. 113–133, 1984.
[11] M. Autret, R. Bernard, and D. Vidal-Madjar, "Theoretical study of the sensitivity of the microwave backscattering coefficient to the soil surface parameters," *Int. J. Remote Sensing,* vol. 10, pp. 171–179, 1989.
[12] B. Brisco, R. J. Brown, B. Snider, G. J. Sofko, J. A. Koehler, and A. G. Wacker, "Tillage effects on the radar backscattering coefficient of grain stubble fields," *Int. J. Remote Sensing,* vol. 12, pp. 2283–2298, 1991.
[13] C. Schmullius and R. Furrer, "Some critical remarks on the use of C-band radar data for soil moisture detection," *Int. J. Remote Sensing,* vol. 13, pp. 3387–3390, 1992.
[14] M. S. Moran, A. Vidal, D. Troufleau, J. Qi, T. R. Clarke, P. J. Pinter, Jr., T. Mitchell, Y. Inoue, and C. M. U. Neale, "Combining multifrequency microwave and optical data for farm management," *Remote Sens. Environ.,* to be published.
[15] X. Huang and Y. Jin, "A simple method to estimate the soil wetness and surface roughness by using active/passive microwave data," *Remote Sens. Environ.,* vol. 53, pp. 212–214, 1995.
[16] E. Attema and F. Ulaby, "Vegetation modeled as a water cloud," *Radio Sci.,* vol. 13, pp. 357–364, 1978.
[17] A. K. Fung, Z. Lee, and K. S. Chen, "Backscattering from a randomly rough dielectric surface," *IEEE Trans. Geosci. Remote Sensing,* vol. 30, pp. 356–369, 1992.
[18] E. Altese, O. Bolognani, M. Mancini, and P. Troch, "Retrieving soil moisture over bare soil from ERS 1 synthetic aperture radar data: Sensitivity analysis based on a theoretical surface scattering model and field data," *Water Resources Res.,* vol. 32, pp. 653–661, 1996.
[19] R. D. Jackson and A. R. Huete, "Interpreting vegetation indices," *J. Veterinary Med.,* vol. 11, pp. 185–200, 1991.

M. Susan Moran received the B.A. degree in geography from San Diego State University, San Diego, CA, in 1976, the M.A. degree in geography from the University of California, Santa Barbara, in 1982, and the Ph.D. degree in soil and water science from the University of Arizona, Tucson, in 1990.

Since 1984, she has been employed as a Physical Scientist with the USDA Agricultural Research Service U.S. Water Conservation Laboratory, Phoenix, AZ. She is also an Adjunct Professor in the Department of Soil, Water, and Environmental Science at the University of Arizona. Her research has focused on theoretical and practical studies of spectral reflectance and emittance from crops and rangelands and related detection of physical and biological stress in vegetation. She is particularly interested in applications of multispectral (optical and microwave) remote sensing for management of both agricultural and wildland resources.

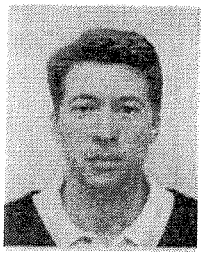

Alain Vidal graduated as an Agricultural and Environmental Engineer from ENGREF, Montpellier, France, in 1985 and received the Ph.D. degree in water sciences and remote sensing from the University of Montpellier, France, in 1989.

He was Project Leader from 1988 to 1992 and then Research Leader at the Cemagref-ENGREF Remote Sensing Laboratory, Montpellier, from 1992 to 1996, and is presently Senior Scientist at the Cemagref Irrigation Division in charge of International Network and of Remote Sensing and GIS applications. His expertise is mainly in bioclimatology, land surface fluxes, and remote sensing applied to irrigation management to forest fire risk assessment. He is a specialist in thermal infrared and optical-microwave synergy in remote sensing.

Dr. Vidal is Vice-Chairman of the French National Committee on Irrigation and Drainage AFEID.

Denis Troufleau received the Engineer degree in agronomy and the B.S. degree in soil and bioclimate sciences from Institut National Agronomique, Paris-Grignon, France, in 1991. He received the Ph.D. degree in hydrological sciences from Ecole National du Génie Rural des Eaux et des Forêts, France, in 1996.

He worked the past few years at LCT Cemagref-ENGREF and ORSTOM, Montpellier, France, on soil moisture and energy balance monitoring at local scale in arid and semi-arid regions from combined thermal infrared/radar data. He is currently working as a Post-Doctoral Scientist at the Institute of Geography, Copenhagen, Denmark, on a mesoscale study of the Sahelian land cover and climate change, with special emphasis on soil moisture, evapotranspiration, and net primary production monitoring from the NOAA Pathfinder data set.

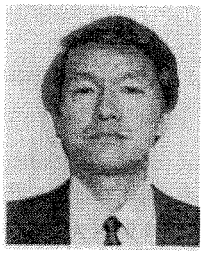

Yoshio Inoue received the B.S. and M.S. degrees in mechanical engineering in 1976 and 1978, respectively, and the M.S. and the Ph.D. degrees in crop science all from Kyoto University, Kyoto, Japan.

He has been with the National Institute of Agro-Environmental Sciences, Tsukuba, Japan, since 1981. He also currently serves as an Adjunct Professor in agricultural engineering at the University of Tsukuba, Tsukuba, Japan. His research has been involved in the interdisciplinary areas of plant physiology, agricultural meteorology, and remote sensing. He is interested especially in the ecophysiological analysis, remote sensing/nondestructive measurements, and simulation-modeling of plant and environmental dynamics in the open field.

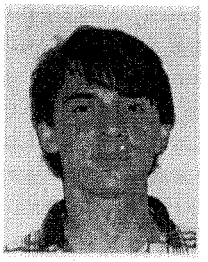

Thomas A. Mitchell received the B.S.E.E. degree from Worcester Polytechnic Institute, Worcester, MA, in 1991 and is currently pursuing the M.S. degree in optics at the Optical Science Center, University of Arizona, Tucson.

He is currently employed by the Hughes Missile Systems Co., Tucson. His main research interests are optical component design and optical system engineering.